

## Competition between two frequencies for phase synchronization of a chaotic laser

Ryan McAllister,<sup>1,2,3</sup> Riccardo Meucci,<sup>4</sup> David DeShazer,<sup>1,2</sup> and Rajarshi Roy<sup>1,2,3,5</sup>

<sup>1</sup>Department of Physics, University of Maryland, College Park, Maryland 20742

<sup>2</sup>IREAP, University of Maryland, College Park, Maryland 20742

<sup>3</sup>CESAR, Computing and Computational Sciences Directorate, Oak Ridge National Laboratory, Oak Ridge, Tennessee 37831-6355

<sup>4</sup>Istituto Nazionale di Ottica Applicata, Largo E. Fermi 6, I-50125 Firenze, Italy

<sup>5</sup>IPST, University of Maryland, College Park, Maryland 20742

(Received 26 June 2002; published 16 January 2003)

Competition between two distinct driving frequencies to phase synchronize the intensity dynamics of a chaotic laser has been observed. The phase of the chaotic intensity signal is constructed using the complex analytic signal. Competing frequencies alternately show phase locking and phase slipping. Competition has been quantified by calculating the portion of time the laser phase locks to each of the driving frequencies and their average.

DOI: 10.1103/PhysRevE.67.015202

PACS number(s): 05.45.Xt, 05.45.Ac, 42.65.Sf, 05.45.Tp

A chaotic system often responds in a complicated way to external driving signals. One such response is phase synchronization, where the amplitudes of response and drive may be poorly correlated, but a relationship becomes evident if suitable phases are defined [1–3].

Phase synchronization of a chaotic system to a single external periodic drive [1,2,4,5] as well as to another chaotic system [3,6,7] has been observed in numerical models and laser experiments. Phase synchronization of chaos is also known to be important in many biophysical phenomena, including brain function [8], kidney function [9], and cardiorespiratory synchronization [10].

In a recent paper [11], Breban and Ott addressed the natural question of how phase synchronization manifests itself when a chaotically behaving system is driven by two regular signals of different periods. The phenomena they found include synchronization to one or the other of the driving frequencies, synchronization to the average frequency, and competition (alternating locking and slipping) between these.

In this paper, we report investigations of phase synchronization in a chaotic laser driven by two sinusoidal signals. We think of this laser as a generic, low-dimensional chaotic system. We observe and quantify competition between the two frequencies and their average for synchronization of the laser. Our results give experimental realizations of the phenomena predicted in Ref. [11].

Our system is the laser with feedback shown in Fig. 1. The laser consists of a diode laser pump source, a neodymium-doped yttrium aluminum garnet (Nd:YAG) laser crystal, an intracavity acousto-optic modulator (AOM), and an output coupler. The laser intensity is detected by a photodiode and the photodiode voltage is applied through a feedback loop to the AOM. The laser operates in a (transverse electromagnetic) TEM<sub>00</sub> Gaussian transverse mode but is free to lase in multiple longitudinal modes.

The AOM modulates the cavity loss around its median value  $k_0$ . The cavity loss induced by the modulator is proportional to  $\sin^2(\pi V/V_{mod})$ , where  $V$  is the voltage applied to the modulation input of the AOM driver and  $V_{mod} = 0.5$  V is the saturation voltage of the driver. The laser is pumped at a ratio of pump power to laser threshold of  $\approx 1.9$ .

The gain  $\Gamma$  and bias  $B$  of the feedback loop can be used to select among a variety of laser dynamics [12]. We tune  $\Gamma$  and  $B$  to a region where the intensity displays chaotic spiking with both irregular spike heights and irregular interspike intervals.

The feedback loop also includes a differential amplifier, with bandwidth  $\beta = 100$  kHz. The output of an arbitrary function generator (40 M samples/s, 12 bits output resolution) can be added to the feedback signal through this amplifier.

Measurements of the photodiode signal are made with a digital oscilloscope with 14 bits of precision. We choose to perform measurements at 5 M samples/s to allow for a well-resolved construction of the Hilbert phase.

Figure 2(a) shows a sample of the chaotic intensity dynamics of the laser with feedback but in the absence of modulation. Among the many options, we turn to the analytic signal to construct a phase for the irregular oscillations [3].

For any real time series  $V^{(r)}(t)$ , such as the laser intensity, we can compute the corresponding analytic signal  $V(t) = V^{(r)}(t) + iV^{(i)}(t)$ , where  $V^{(i)} \equiv \pi^{-1} P \int_{-\infty}^{\infty} V^{(r)}(t') (t'$

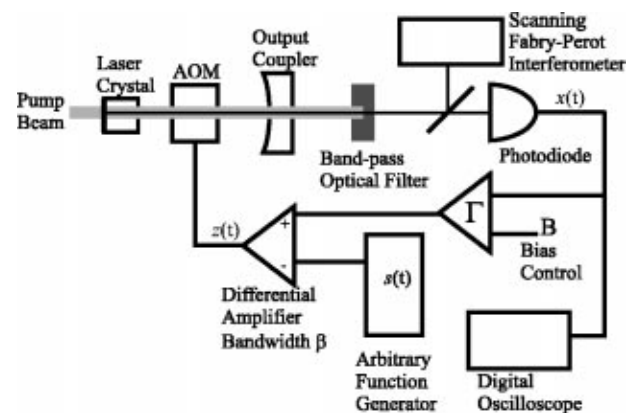


FIG. 1. Experimental setup of a diode-pumped Nd:YAG laser with an intracavity AOM. The solid line connecting the detector to the AOM indicates the feedback loop generating the chaotic dynamics. A signal  $s(t)$  from the arbitrary function generator may be added to the voltage in the feedback loop.

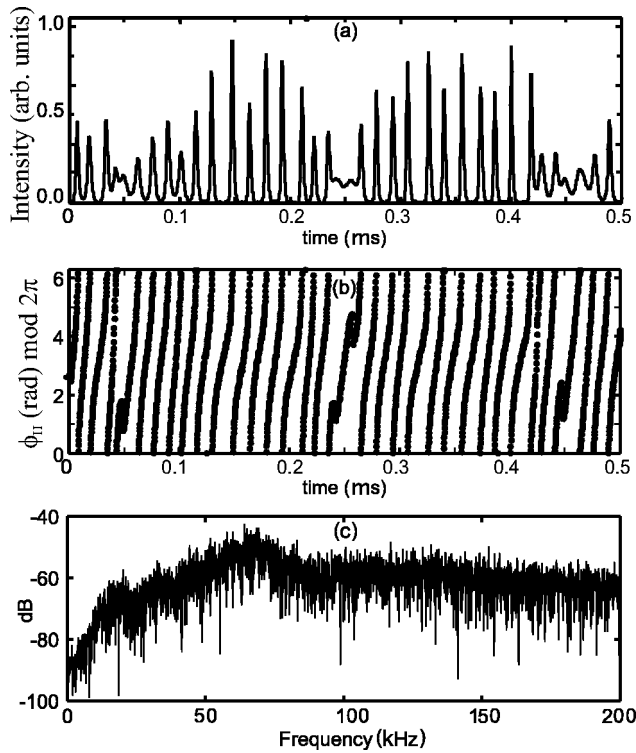


FIG. 2. (a) Time series recorded from the laser with feedback but no modulation. (b) The reconstructed phase of the signal from (a), modulo  $2\pi$ . (c) Power spectrum of the laser. The spectrum is broad and its highest peak is at  $\approx 64$  kHz. We can also perceive what appear to be 1:2 and 1:3 subharmonic peaks at 32 kHz and 21 kHz, respectively.

$-t)^{-1}dt'$  is the Hilbert transform of  $V^{(r)}(t)$  and  $P$  denotes taking the principal value of the integral. Writing  $V(t) = A(t)e^{i\phi_H(t)}$ , where  $A(t)$  is a real function, we obtain the Hilbert phase  $\phi_H(t)$  of the real signal  $V^{(r)}(t)$ . This phase describes changes in the field envelope and can be evaluated from experimental time series using the fast Fourier transform [13].

Figure 2(b) shows the Hilbert phase constructed from the signal shown in Fig. 2(a). The constructed phase  $\phi_H$  corresponds in a sensible manner with the recorded dynamics of the laser intensity.

The power spectrum of the laser in the same conditions is displayed in Fig. 2(c). The main peak in the power spectrum ( $\approx 64$  kHz) is close to the relaxation oscillation frequency  $f_{rel}$  of the laser dynamics.

Beyond the range of frequency displayed, the power spectrum of the recorded laser intensity signal decays exponentially with respect to frequency down to the 14 bit resolution of the digital oscilloscope.

We now add a single-frequency sinusoidal perturbation onto the voltage feedback signal. For sufficient amplitude and for choices of  $f$  close to the relaxation oscillation frequency, the phase of the chaotic signal typically synchronizes intermittently to the perturbation. The laser intensity remains chaotic unless the perturbation becomes large compared to the feedback signal ( $\approx 90$  mV peak to peak), where

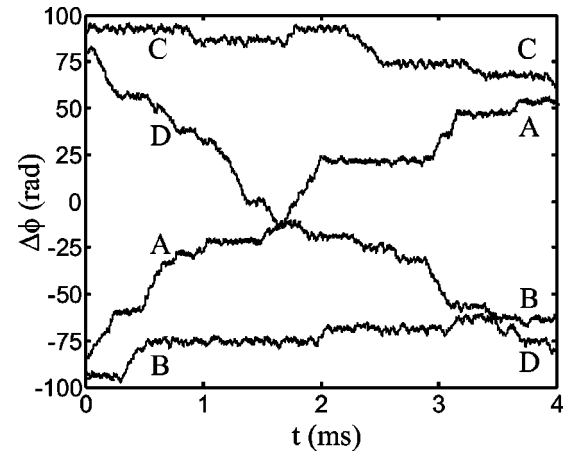


FIG. 3.  $\Delta\phi$  from the experimental system for four values of a single driving frequency. The AOM is driven with an amplitude of 50 mV. In the four curves, we can see long plateaus of synchronization as well as large phase slips. Curve A;  $f = 50.0$  kHz, Curve B;  $f = 60.0$  kHz, Curve C;  $f = 67.8$  kHz, Curve D;  $f = 74.9$  kHz.

the intensity dynamics consists of regular spikes fully entrained to the driving frequency.

We consider the constructed phase  $\phi_H(t)$  of the chaotic laser intensity signal as unbounded (not taken modulo  $2\pi$ ) and define  $\Delta\phi$  for the chaotic signal with respect to a given frequency  $f$  as

$$\Delta\phi(t) = \phi_H - 2\pi ft. \quad (1)$$

In Fig. 3, we display the phase difference  $\Delta\phi$  between the sinusoidal modulation and the chaotic signal for four values of the driving frequency  $f$ . When  $f$  is below the laser relaxation oscillation frequency  $f_{rel}$ , phase slips occur predominantly with the phase of the laser advancing more quickly than that of the driving (slanted segments of  $\Delta\phi$  with positive mean slope). When  $f$  is above  $f_{rel}$ , phase slips tend to occur in the other direction. Nearly horizontal segments of  $\Delta\phi$  represent times during which the laser has become phase synchronized to the sinusoidal modulation. With similar amplitudes, driving frequencies closer to  $f_{rel}$  tend to entrain the laser phase for longer periods of time than frequencies further from  $f_{rel}$ .

The phases of the chaotic signals in all four curves synchronize to the perturbation for intervals as long as several tenths of a millisecond, or many times the characteristic period of the laser relaxation oscillations. During these intervals of synchronization,  $\Delta\phi$  wiggles irregularly due to the varying shape of the intensity oscillations but remains within a range of width  $2\pi$ .

When we introduce driving composed of sinusoids at two frequencies, we are able to observe competition for synchronization between each of the frequencies ( $f_1, f_2$ ) and their average ( $f_{av}$ ).

For periods of time containing tens or hundreds of oscillations of intensity, the laser can phase synchronize to one frequency, say  $f_i$ . During this time, the line representing  $\Delta\phi_i = \phi_H - 2\pi f_i t$  will look flat if one ignores fluctuations of magnitude less than  $2\pi$ . At the same time, the lines repre-

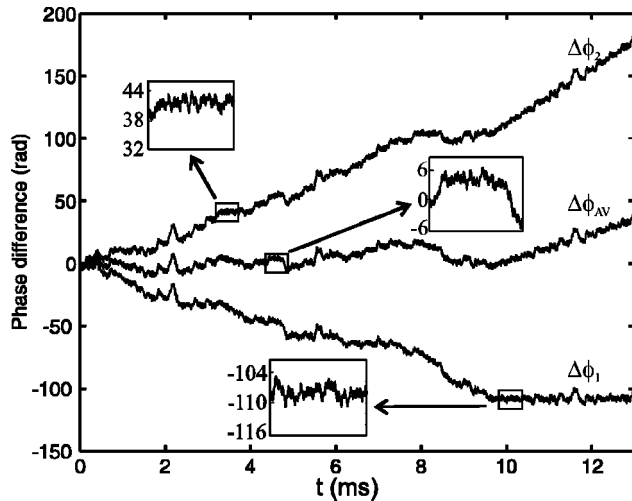


FIG. 4.  $\Delta\phi$  for the experiment with two driving frequencies  $f_1 = 62.5$  kHz and  $f_2 = 59.0$  kHz, both with an amplitude of 50 mV. The top curve represents  $\Delta\phi_2$ , which tends to increase with time, the bottom curve represents  $\Delta\phi_1$ , which tends to decrease with time, and the middle curve represents  $\Delta\phi_{av}$ . The inset boxes display enlarged sections of the three  $\Delta\phi$  curves, each over a time of 0.5 ms.

senting the phase differences between the chaotic laser intensity signal and the other two frequencies will slant down or up, depending upon whether each frequency is greater or lesser than the frequency that is successfully entraining the chaotic dynamics.

Figure 4 shows a plot of the phase differences for  $f_1$ ,  $f_2$ , and  $f_{av}$  in an experimental run with two-frequency modulation. The two driving frequencies in this case are slightly lower than the relaxation oscillation frequency, and the amplitude of the perturbation is chosen so that entrainment is observed while chaos is preserved. Each inset enlarges a segment during which the phase of the laser signal is entrained dominantly to one of  $f_1$ ,  $f_2$ , or  $f_{av}$ . Surprisingly, the laser predominantly slips back and forth between synchronization to  $f_2$  and  $f_{av}$ , even though  $f_1$  is closer to  $f_{rel}$ , see Fig. 5.

Following Ref. [11], we plot  $\Delta\phi_2$  vs  $\Delta\phi_1$  from the data in Fig. 4 as curve A in Fig. 5. The staircaselike structure we observe shows that  $\Delta\phi_1$  is typically locked (within  $2\pi$ ) while  $\Delta\phi_2$  slips (vertical segments), and  $\Delta\phi_2$  is typically locked while  $\Delta\phi_1$  slips (horizontal segments). Line segments with slope close to +1 indicate that the phase of the chaotic signal is slipping with respect to both of the driving frequencies. As  $f_1$  and  $f_2$  are unequal, the slope cannot be exactly +1.

We create a piecewise linear simplification of each  $\Delta\phi$  curve by inspection. The simplification is composed of line segments of zero slope with slanted segments connecting them. The total length of line segment of slope zero within a particular  $\Delta\phi_i$  curve is counted as synchronization to  $f_i$ . The portion of time the laser spends phase synchronized to each frequency has been calculated this way and entered in Table I.

Curves B and C in Fig. 5 show similar behaviors, typically seen for driving at frequencies above, below, or straddling

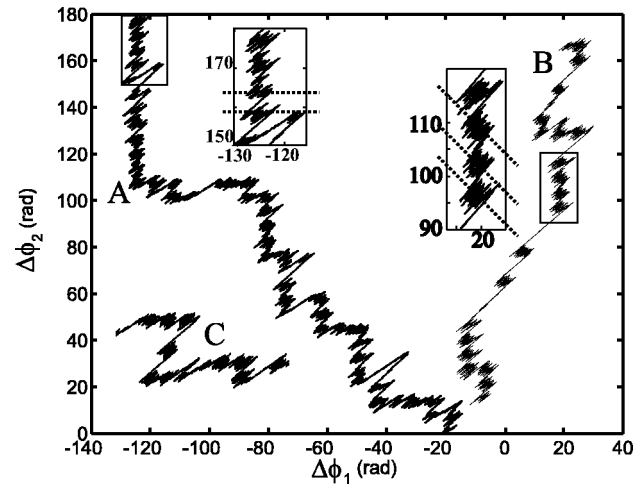


FIG. 5.  $\Delta\phi_2$  vs  $\Delta\phi_1$  for three experimental time series with different driving. Phase synchronization to  $f_1$  appears as vertical trails, synchronization to  $f_2$  appears as horizontal trails. Curve A; the same 13 ms time series as in Fig. 4. The inset shows that during the long time apparently synchronized to  $f_1$ , the phase is often in fact synchronized to  $f_{av}$  or  $f_2$ . Curve B; a 13 ms time series with  $f_1 = 59.0$  kHz,  $f_2 = 57.5$  kHz. Synchronization to the average can be seen when  $\Delta\phi_1$  increases while  $\Delta\phi_2$  decreases, as in the inset. Curve C; a 6.5 ms time series where both frequencies are greater than the relaxation oscillation frequency of the laser,  $f_1 = 67.9$  kHz,  $f_2 = 66.0$  kHz.

the laser relaxation oscillation frequency  $f_{rel}$  ( $\approx 64$  kHz). In curve B, climbing from bottom to top, synchronization to the average is most prevalent and seems to occur repeatedly for short stretches where  $\Delta\phi_1$  and  $\Delta\phi_2$  also vary by less than  $2\pi$ . These stretches of synchronization to  $f_{av}$  appear as short sequences with an average slope of  $-1$ , as in the inset. In curve C, the driving frequencies are greater than  $f_{rel}$ , also in this case, the net slip in phase is least. In all the three cases, the net chaotic phase slip is least with respect to the driving frequency closest to  $f_{rel}$ , even if the chaotic phase locks more often to the other frequency or  $f_{av}$ . The portion of time that the intensity signal stays phase locked for all two-frequency data are displayed in Table I.

One might also try to detect phase synchronization by examining the spectrogram. However, discerning synchronization over short times requires a small time window for the calculation of the spectrum, while achieving high resolution in frequency requires a longer time window. Therefore, it is difficult to observe competition between two frequencies with a spectrogram when the durations of synchronization may be short and the frequencies of interest may be close together.

TABLE I. The portion of time each of the three plots of  $\Delta\phi_2$  vs  $\Delta\phi_1$  displayed in Fig. 5 phase locks to one of  $f_1$ ,  $f_2$ , and  $f_{av}$ .

Curve	$f_1$ (kHz)	$f_2$ (kHz)	to $f_1$	to $f_2$	to $f_{av}$	Slipping
A	62.5	59.0	0.06	0.34	0.21	0.39
B	59.0	57.5	0.01	0.08	0.68	0.22
C	67.9	66.0	0.12	0.31	0.27	0.30

We have also tried to detect phase synchronization by examining a three-dimensional time-delay embedding of the attractor. However, we discover that trajectories within the attractors corresponding to synchronization to  $f_1$ ,  $f_{av}$ , or  $f_2$  are visually indistinguishable from each other. Thus it is not clear how to determine to which frequency the dynamics is phase locked by examining the attractor. On the other hand, phase slips tend to occur in the region of low intensity when all three phase differences are advancing, and of high intensity when all three phase differences are decreasing.

We have observed phase synchronization of the intensity dynamics of a chaotic laser driven by two periodic signals at different frequencies. The laser phase alternately locks and slips between synchronization to the two driving frequencies and their average. These behaviors predicted in Ref. [11] can be seen and distinguished by plotting one phase difference against the other, even though they are difficult to discern by examining the attractor or a spectrogram. We believe this to

be an experimental observation of a very general phenomenon for nonlinear systems driven by more than one frequency.

#### ACKNOWLEDGMENTS

This research was supported in part by the U.S. Department of Energy, Office of Basic Energy Sciences. The Oak Ridge National Laboratory is managed for the U.S. Department of Energy by UT-Battelle, LLC, under Contract No. DE-AC05-00OR22725. We also gratefully acknowledge support from the Office of Naval Research (Physics). R. Meucci also wishes to acknowledge the European Contract No. HPRN-CT-2000-00158 for supporting his visit to the University of Maryland. We thank Romulus Breban and Ed Ott for inspiring this study and Yuri Braiman for helpful discussions. We are also thankful for expert technical assistance from Don Martin.

- 
- [1] A.S. Pikovsky, *Sov. J. Commun. Technol. Electron.* **30**, 85 (1985).
- [2] E.F. Stone, *Phys. Lett. A* **163**, 367 (1992).
- [3] M.G. Rosenblum, A.S. Pikovsky, and J. Kurths, *Phys. Rev. Lett.* **76**, 1804 (1996).
- [4] E. Allaria, F.T. Arecchi, A. Di Garbo, and R. Meucci, *Phys. Rev. Lett.* **86**, 791 (2001).
- [5] A.S. Pikovsky, M.G. Rosenblum, G.V. Osipov, and J. Kurths, *Physica D* **104**, 219 (1996).
- [6] K.V. Volodchenko *et al.*, *Opt. Lett.* **26**, 1804 (2001).
- [7] D.J. DeShazer, R. Breban, E. Ott, and R. Roy, *Phys. Rev. Lett.* **87**, 044101 (2001).
- [8] M. Le Van Quyen *et al.*, *J. Neurosci. Methods* **111**, 83 (2001).
- [9] D.E. Postnov, O.V. Sosnovtseva, E. Mosekilde, and N.-H. Holstein-Rathlou, *Int. J. Mod. Phys. B* **15**, 3079 (2001); N.-H. Holstein-Rathlou, K.-P. Yip, O.V. Sosnovtseva, and E. Mosekilde, *Chaos* **11**, 417 (2001).
- [10] D. Hoyer *et al.*, *IEEE Eng. Med. Biol. Mag.* **20**, 101 (2001); C. Schafer, M.G. Rosenblum, J. Kurths, and H.-H. Abel, *Nature (London)* **392**, 239 (1998); C. Schafer, M.G. Rosenblum, H.-H. Abel, and J. Kurths, *Phys. Rev. E* **60**, 857 (1999).
- [11] R. Breban and E. Ott, *Phys. Rev. E* **65**, 056219 (2002).
- [12] R. Meucci, R. McAllister, and R. Roy, *Phys. Rev. E* **66**, 026216 (2002).
- [13] D. Gabor, *J. IEE (London)* **93**, 429 (1946); M. Born and E. Wolf, *Principles of Optics*, 7th ed. (Cambridge University Press, Cambridge, New York, 1999), pp. 557–562.